Exposure to diphtheria toxin during the juvenile period impairs both inner and outer hair cells in C57BL/6 mice

Hiroyuki Konishi[a], Nobutaka Ohgami[b,c], Aika Matsushita[a], Yuki Kondo[a], Yuki Aoyama[d], Masaaki Kobayashi[a], Taku Nagai[d], Shinya Ugawa[e], Kiyofumi Yamada[d], Masashi Kato[b], Hiroshi Kiyama[a]

[a]Department of Functional Anatomy and Neuroscience, Nagoya University Graduate School of Medicine, Nagoya, 466-8550, Japan

[b]Department of Occupational and Environmental Health, Nagoya University Graduate School of Medicine, Nagoya, 466-8550, Japan

[c]Nutritional Health Science Research Center, Chubu University, Kasugai, 487-8501, Japan

[d]Department of Neuropsychopharmacology and Hospital Pharmacy, Nagoya University Graduate School of Medicine, Nagoya, 466-8550, Japan

[e]Department of Anatomy and Neuroscience, Graduate School of Medical Sciences, Nagoya City University, Nagoya, 467-8601, Japan

E-mail addresses:

Hiroyuki Konishi: konishi@med.nagoya-u.ac.jp

Nobutaka Ohgami: nobugami@med.nagoya-u.ac.jp

Aika Matsushita: aika.mat@hotmail.co.jp

Yuki Kondo: kondogagigugego@gmail.com

Yuki Aoyama: y.aoyama1007@gmail.com

Masaaki Kobayashi: 4444.forum@gmail.com

Taku Nagai: t-nagai@med.nagoya-u.ac.jp

Shinya Ugawa: ugawa@med.nagoya-cu.ac.jp

Kiyofumi Yamada: kyamada@med.nagoya-u.ac.jp

Masashi Kato: katomasa@med.nagoya-u.ac.jp

Hiroshi Kiyama: kiyama@med.nagoya-u.ac.jp

Corresponding author:

Hiroyuki Konishi or Hiroshi Kiyama, Department of Functional Anatomy and Neuroscience, 65 Tsurumai-cho, Showa-ku, Nagoya 466-8550, Japan, Tel.: +81-52-744-2015, Fax: +81-52-744-2027, E-mail: konishi@med.nagoya-u.ac.jp, kiyama@med.nagoya-u.ac.jp

Abbreviations:

ABR, auditory brainstem response

DT, diphtheria toxin

DTR, DT receptor

EDTA, ethylenediaminetetraacetic acid

EF-2, elongation factor-2

HB-EGF, heparin-binding epidermal growth factor-like growth factor

HC, hair cell

H&E, hematoxylin and eosin

IHC, inner hair cell

OHC, outer hair cell

P, postnatal

PB, phosphate buffer

PBS, phosphate-buffered saline

PFA, paraformaldehyde

SEM, scanning electron microscopy

SGN, spiral ganglion neuron

SPL, sound pressure level

SV, stria vascularis

TNBT, tetranitro blue tetrazolium

W, week-old

WT, wildtype

ABSTRACT

Diphtheria toxin (DT) administration into transgenic mice that express the DT receptor (DTR) under control of specific promoters is often used for cell ablation studies *in vivo*. Because DTR is not expressed in mice, DT injection has been assumed to be nontoxic to cells *in vivo*. In this study, we demonstrated that DT application during the juvenile stage leads to hearing loss in wildtype mice. Auditory brainstem response measurement showed severe hearing loss in C57BL/6 mice administered DT during the juvenile period, and the hearing loss persisted into adulthood. However, ototoxicity did not occur when DT was applied on postnatal day 28 or later. Histological studies demonstrated that hearing loss was accompanied by significant degeneration of inner and outer hair cells (HCs), as well as spiral ganglion neurons. Scanning electron microscopy showed quick degeneration of inner HCs within 3 days and gradual degeneration of outer HCs within 1 week. These results demonstrated that DT has ototoxic action on C57BL/6 mice during the juvenile period, but not thereafter, and the hearing loss was due to degeneration of inner and outer HCs by unknown DT-related mechanisms.

Keywords: cochlea; degeneration; diphtheria toxin; hair cell; hearing loss; ototoxicity

Conditional ablation of specific cells is an indispensable technique for studying cellular functions *in vivo*. In recent studies, transgenic or knock-in mice, which are designed to express diphtheria toxin (DT) receptor (DTR) in a specific cell-type, have been used for conditional ablation studies (Saito et al., 2001). DT is an exotoxin secreted by *Corynebacterium diphtheriae*. After binding to DTR, which is identical to human heparin-binding epidermal growth factor-like growth factor (HB-EGF) (Naglich et al., 1992), DT is translocated to endosomes by endocytosis, and the A-fragment of DT is released into the cytoplasm (Collier and Kandel, 1971; Gill and Dinius, 1971; Dorland et al., 1979). The released A-fragment then catalyzes ADP-ribosylation of elongation factor-2 (EF-2) and inhibits protein synthesis, thereby inducing cell death (Honjo et al., 1968; Robinson et al., 1974). The DT-induced ablation system in mice is based on the fact that DT binds to human HB-EGF but not to mouse HB-EGF (Mitamura et al., 1995; Cha et al., 1998). Mice have been shown to be resistant to DT (Pappenheimer et al., 1982), and conditional ablation of specific cells, which exogenously express DTR, is achieved by systemic administration of DT (Saito et al., 2001).

Because DT itself is assumed to have no biological effect on wildtype (WT) mice, several studies failed to include a control group that treated WT mice with DT in their study (Kwon et al., 2014; Wang et al., 2014). Conversely, some studies have reported unexpected off-target effects of DT on WT mice, such as weight loss (Meyer Zu Horste et al., 2010; Goldwich et al., 2012; Christiaansen et al., 2014), proteinuria (Goldwich et al., 2012), and mucosal inflammation of the lung (Chapman and Georas, 2013). Furthermore, high-dose DT was shown to be lethal in mice (Bonventre et al., 1973; Goldwich et al., 2012; Christiaansen et al., 2014). Because these reports used purified DT with few contaminants, such as endotoxins, and demonstrated consistent results using DT supplied from different vendors (Meyer Zu Horste et al., 2010; Chapman and Georas, 2013; Christiaansen et al., 2014), these studies demonstrated that DT causes adverse effects on mice.

In an analysis using DTR knock-in mice from the C57BL/6 strain, results unexpectedly showed that DT-treated juvenile mice exhibited abnormal behaviors in response to auditory stimuli, and this abnormality was also observed in C57BL/6 WT mice. Therefore, we hypothesized that DT might induce side effects, such as hearing loss. In the present study, we investigated the effects of DT during postnatal development, and results revealed that inner hair cells (IHCs), outer hair cells (OHCs), and spiral ganglion neurons (SGNs) were impaired after DT treatment, and juvenile C57BL/6 mice were more susceptible to DT.

EXPERIMENTAL PROCEDURES

Animals

Male C57BL/6J and CBA/J mice were purchased from Charles River Laboratories Japan (Yokohama, Japan). All experimental procedures were conducted in accordance with standard guidelines for animal experiments from the Nagoya University Graduate School of Medicine. This study was approved by the local animal ethics committee of Nagoya University (approval number: 26181, 27204 and 28303). All efforts were made to minimize the number of animals and their suffering.

Recording of auditory brainstem response (ABR)

Phosphate-buffered saline (PBS) or DT (50 µg/kg, Sigma, St Louis, MO, USA) was intraperitoneally injected into postnatal (P) 7, P14, P28, or 8-week-old (W) mice. Survival rates were almost 100%, and neither morphological nor behavioral abnormalities were observed after treatment with this DT dose. ABR was measured as described in our previous reports at 14 or 15 days after DT administration (AD Instruments Pty. Ltd., Castle Hill, Australia) (Ohgami et al., 2010). Tone-burst stimuli at 4, 12, 20, and 32 kHz were recorded in 10-dB increments from 0 to 90 or 100 dB sound pressure level (SPL). The threshold was determined by identifying the lowest level of wave I. When any wave was not observed at the highest stimulation level, the threshold was assigned to the highest presentation level plus 10 dB. The number of “scale-out” animals is indicated in each figure. In control mice, the thresholds were higher than previous reports, in particular at high frequency, which could be due to our ABR system setup.

Hematoxylin and eosin (H&E) staining and quantification of SGN numbers

Mice were intraperitoneally injected with PBS or DT (50 μg/kg) at P7. At P21 or P56, mice were anesthetized and perfused with 4% paraformaldehyde (PFA) in 0.1 M phosphate buffer (PB). Inner ears were dissected, post-fixed in the same fixative overnight at 4°C, and decalcified in 0.1 M PB containing 10% ethylenediaminetetraacetic acid (EDTA) for several days. The 5-μm-thick paraffin sections were cut on a microtome, deparaffinized with xylene, and then stained with H&E. After dehydration with an ascending ethanol series, sections were cleared with xylene and mounted. The number of SGNs in the apical, middle and basal turn were quantified and normalized to the spiral ganglion area. A total of 9 sections from 3 animals (3 sections per animal) were analyzed at each time point. The interval of each section was at least 30 μm, and there was no possibility of double-counting the same cells.

Whole-mount tetranitro blue tetrazolium (TNBT) staining of the cochlea

Mice were intraperitoneally injected with PBS or DT (50 μg/kg) at P7 and HC numbers were analyzed at P21. TNBT staining of cochlea was performed in accordance with a previous report (Wang et al., 2011). Briefly, cochleae were dissected and incubated in a staining solution containing sodium succinate and TNBT for 45 min at 37°C. After fixation with 10% formalin, the bone was carefully removed from the apex using fine forceps, and images of the HC surface were taken by a stereoscopic microscope M60 (Leica Microsystems, Wetzlar, Germany) at the apical, middle, and basal turn. The number of IHCs and OHCs were quantified in each turn and normalized to the length of the basilar membrane. Five animals were analyzed in total.

Scanning electron microscopy (SEM)

Mice intraperitoneally injected with PBS or DT (50 µg/kg) at P7 were analyzed by SEM at P8, 10, 14, and 21. After decapitation, the inner ear was dissected and immediately immersed in a fixative (30 mM HEPES, pH 7.4, 5% glutaraldehyde, 10% PFA, 100 mM NaCl, 2 mM $CaCl_2$). The cochleae were perfused with the fixative, post-fixed in the same fixative for 1 week, and decalcified in 0.1 M PB (pH 6.6) containing 8% EDTA, 4% PFA, and 10% sucrose for at least 3 days. Then the cochleae were processed using the osmium tetroxide and thiocarbohydrazide method (Hunter-Duvar, 1978). After dehydration with a critical point dryer (EM CPD300, Leica Microsystems), images of the middle turn were taken by an electron microscope (JSM-7610F, JEOL Ltd, Tokyo, Japan) with a magnification of 2,000× or 15,000×. At least three animals were analyzed and representative images are shown.

Statistical analyses

Values are expressed as mean ± S.E.M. Data were analyzed using Student's *t*-test, and $P < 0.05$ was considered statistically significant.

RESULTS

Hearing impairment is observed in C57BL/6 WT mice treated with DT during the juvenile period

We intraperitoneally injected DT into P7 C57BL/6 WT mice at a dose of 50 μg/kg. The same or a greater dose was generally used to ablate DTR-expressing cells in the brain *in vivo* (Knowlton et al., 2013; Parkhurst et al., 2013; Pedersen et al., 2013). Survival rates were nearly 100%, and visible morphological or behavioral abnormalities were not observed after DT treatment. However, severe hearing loss developed in the DT-treated mice at P21 (14 days after DT administration) (Fig. 1A and B). ABR measurements, which recorded electrical signals evoked from the brainstem by sound stimuli, demonstrated that ABR thresholds were significantly greater in DT-treated mice at all frequencies. To examine the possibility that hearing impairment was transient, the same mice were allowed to mature to adult (8W) and the ABR test was repeated (Fig. 1C). Hearing loss was consistently observed in the adult mice, suggesting that the hearing loss was permanent.

In several previous studies using DT, behavioral tests, such as fear conditioning and pre-pulse inhibition that uses sound, were normal in DT-treated mice (Han et al., 2009; Xu et al., 2015). Because those studies used adult mice, we hypothesized that DT-induced hearing loss might depend on the developmental stage at DT administration. Therefore, we injected DT into C57BL/6 mice at P14, P28, and adult (8W), and measured ABR at 14 or 15 days after injection (Fig. 2). Similar or more severe hearing loss was also observed in P14-administrated mice (Fig. 2A). When we applied DT at P28, hearing levels slightly declined. However, the decreased level was not statistically significant at all frequencies (Fig. 2B). The ABR threshold after DT administration at 8W showed comparable patterns with the vehicle-injected mice (Fig. 2C). These results indicated that juvenile mice were more susceptible to damage, and suggested the existence of a developmental time window in DT-induced hearing loss. For subsequent studies, we analyzed WT mice that were administered DT at P7.

Loss of SGNs and HCs in DT-treated C57BL/6 mice

To investigate the cause of hearing loss, we first tested H&E staining on cochlear sections (Fig. 3A). C57BL/6 mice administrated DT at P7 were analyzed at P21 and 8W. We found that the SGN density in DT-administrated mice was less in all turns of the cochlear, although no statistical significance was detected in the apical turn at 8W (Fig. 3A and B). Concomitant loss of IHCs and OHCs was evident in many sections in the DT-administrated group (Fig. 3A). To confirm HC loss, we performed whole-mount staining of cochleae with TNBT, which labels both IHCs and OHCs in C57BL/6 mice (Wang et al., 2011). In vehicle-injected cochlea of P21 mice, three lines of OHCs and a single line of IHCs were clearly identified; whereas in DT-treated cochlea, discontinuous and disarrayed lines of IHCs and OHCs were observed (Fig. 3C). Statistical analysis demonstrated a significant decrease in the number of IHCs and OHCs in the apical, middle, and basal turn of the DT-administrated group (Fig. 3D). To further analyze HC loss, we performed SEM on the middle turn at P21, revealing significant loss of IHCs and OHCs, while the surviving cells exhibited relatively normal hair morphology in the DT-treated mice (Fig. 3E). Results from these histological studies suggested that SGN and HC loss might cause hearing impairment.

Time-course study of HC degeneration in C57BL/6 mice

Because HC loss was apparent in P21 C57BL/6 mice administrated with DT at P7, we observed the degeneration process of HCs in the middle turn by SEM between P7 and P21 (Fig. 4). The HC number and morphology were normal, and there was no sign of degeneration at P8 (Fig. 4A–F). However, at P10 (Fig. 4G–L), IHCs were significantly degenerated in the DT-treated mice (Fig. 4G, H, J and K). Additionally, several OHCs exhibited degenerative features with disordered hair as indicated by an arrowhead (Fig. 4G, I, J and L). At P14, many OHCs and IHCs were degenerated in the DT-treated mice (Fig. 4M–R), and the overall image was comparable to that of P21 (Fig. 3E). These results suggested that IHCs quickly degenerated, and a significant number of OHCs gradually degenerated, suggesting that IHCs were more susceptive to DT toxicity than OHCs.

DT ototoxicity in CBA/J mice

Up to this point, we had only analyzed C57BL/6 mice (Fig. 1–4). However, C57BL/6 mice have a homozygous mutation in the cadherin 23 gene, causing severe age-related hearing loss owing to HC degeneration (Noben-Trauth et al., 2003). This suggested the possibility that the ototoxic effect of DT in C57BL/6 mice is a result of accelerated age-related HC degeneration. Therefore, we examined the CBA/J strain (Fig. 5), which does not have the genetic mutation and is highly resistant to age-related hearing loss (Willott, 1986; Ohlemiller et al., 2010). The CBA/J WT mice received the same dose of DT (50 µg/kg) at P7, and we subsequently evaluated hearing ability at P21 by ABR measurements (Fig. 5A). Results showed that DT administration also induced hearing impairment at P21, although the severity was less than in C57BL/6 mice at lower frequencies (Fig. 1 and 2). SEM images of the middle turn at P21 showed significant degeneration of both IHCs and OHCs (Fig. 5B), suggesting that DT ototoxicity was not due to an increased susceptibility to age-related HC loss in C57BL/6 mice.

DISCUSSION

Results from this study demonstrated that HCs and SGNs of C57BL/6 mice are susceptible to DT exposure particularly during the juvenile period. Administration of DT (50 µg/kg, i.p.) caused HC and SGN degeneration in juvenile mice (Fig. 3 and 4), resulting in permanent hearing loss (Fig. 1). IHC degeneration occurred quicker and was more severe than in the OHCs (Fig. 3C–E and 4). HCs are assumed to support SGN survival by secreting neurotrophic factors (Schecterson and Bothwell, 1994; Rubel and Fritzsch, 2002), and a recent study reported that HC degeneration leads to SGN loss in neonatal mice (Tong et al., 2015). Furthermore, our histological results showed that SGN degeneration was milder even at 8W, while HC degeneration was more severe (Fig. 3). Taken together, it is likely that SGN degeneration is due to HC loss.

Because the DTR knock-in mouse strain, which we initially used, was bred onto the C57BL/6 background, we analyzed the side effect of DT in C57BL/6 mice (Fig. 1–4). The C57BL/6 mice develop severe age-related hearing loss due to a homozygous mutation in the cadherin 23 gene (Noben-Trauth et al., 2003). Therefore, we analyzed CBA/J mice (Fig. 5), which do not carry the genetic mutation (Noben-Trauth et al., 2003). Although CBA/J mice do not develop age-related hearing loss at least until 1 year of age (Ohlemiller et al., 2010), significant hearing loss (Fig. 5A) and HC degeneration (Fig. 5B) also occurred in the juvenile CBA/J mice within 14 days after DT administration, suggesting that the C57BL/6 phenotype was not due to accelerated age-related hearing loss (Fig. 5). All of the present data were collected from male mice (Fig. 1–5). However, we also examined female littermates of C57BL/6 mice in our preliminary experiment, and ABR measurements consistently showed hearing loss after DT administration during the juvenile period (data not shown). These results suggested that DT ototoxicity could be a general side effect in mice.

Two recent papers have shown selective IHC degeneration after systemic DT administration in WT mice (Song et al., 2015; Tong et al., 2015), although these studies only reported the phenomenon and did not address the details. Song et al. intraperitoneally administrated DT (50 μg/kg, 3 times) into CBA/CaJ WT mice at 5W, showing a significant loss of IHCs, but intact OHCs (Song et al., 2015). We administrated DT (50 μg/kg, once) into C57BL/6 mice, which resulted in no statistically significant differences in ABR thresholds at P28 (4W) and thereafter (Fig. 2B and C). However, the threshold at P28 exhibited an increased tendency in the DT-treated group (Fig. 2B). The total DT dose used in the Song et al. study was three times higher than in our study, which could explain the HC degeneration observed at 5W in their study. Additionally, the critical periods were slightly different between the strains. Tong et al. also showed that only a small number of IHCs degenerated after intramuscular administration of DT (25 μg/kg) into CBA/J WT mice at P21–P42 (Tong et al., 2015). The dose was half of the dose used in the present study, and the timing of administration overlapped the critical period in C57BL/6 mice (Fig. 2); these results were largely consistent with ours. In the same paper, however, results from the neonatal mice were inconsistent (Tong et al., 2015); both OHCs and IHCs were unaffected by intramuscular administration of DT (4 μg/kg) at P2. This discrepancy was possibly caused by the DT dose. They used a very low dose for the P2 mice, which could account for a lack of ototoxicity. Similarly, three additional studies reported that low-dose DT resulted in no changes in HC morphology in the WT mice (Mahrt et al., 2013; Cox et al., 2014; Kurioka et al., 2016). Although the DT dose could be a critical determinant of the phenotype, as previously discussed, a recent study reported conflicting results (Hu et al., 2016); they intraperitoneally administrated DT (100 ng three times) into C57BL/6 WT mice at P1. Although the higher dose (approximately 4 times higher than ours in total) was used in the Hu et al. study, the HCs remained intact at 3 days after injection. Because HC degeneration onset was between 1 and 3 days after DT administration in our experiment (Fig. 4), ototoxicity might not have been observed when they analyzed HC morphology.

In a DT-induced ablation system using DTR (human HB-EGF) transgenic or knock-in mice, the initial binding of DT to exogenously expressed human HB-EGF is essential, because DT is assumed to have a very low affinity for mouse HB-EGF (Mitamura et al., 1995; Cha et al., 1998). Although it remains unclear why DT induces HC loss, several possibilities can be raised. Given that DT directly binds to and kills HCs, a binding partner is necessary. Results from the present study indicate that DT is toxic to mouse HCs in a human HB-EGF non-mediated manner. Therefore, it is likely that another receptor, which has a higher affinity to DT and is expressed by HCs, exists. To examine the possibility of direct binding of DT to HCs, we preliminarily attempted to utilize a previously described organ culture system (data not shown) (Parker et al., 2010). We isolated the organ of Corti from P7 mice, and cultured the organ with high concentrations of DT. The number of HCs remained unchanged between control and DT-treated groups, even after 7 days *in vitro*, suggesting that DT may not directly bind to receptors on HCs. Thus, HC degeneration may be due to an indirect effect of DT.

Some possibilities should be considered with regard to an indirect effect of DT. Because an impaired endolymphatic system, for instance, causes HC degeneration and occurs in Meniere’s disease (Nakashima et al., 2016), it is possible that DT may damage the stria vascularis (SV) where the endolymph is produced (Patuzzi, 2011). However, we did not observe any SV damages in our preliminary experiments (data not shown). We examined the integrity of the blood-endolymph barrier in the SV at P10 using a transcardial injection of Evans blue dye, which is known to leak after barrier disruption (Zhang et al., 2012). However, we did not detect any extravasation of dye. Furthermore, the number and morphology of perivascular macrophages, which are in close contact with capillaries within the SV and become activated along with blood-endolymph barrier dysfunction (Zhang et al., 2013; Zhang et al., 2015), remained unchanged after DT treatment. Thus, SV damage is unlikely. Another possibility is that changes in peripheral organs may affect HCs and cause secondary degeneration. We systemically injected DT in this study, which could induce some unexpected side effects in peripheral organs. Some previous studies reported lethality (Bonventre et al., 1973; Goldwich et al., 2012; Christiaansen et al., 2014), weight loss (Meyer Zu Horste et al., 2010; Goldwich et al., 2012; Christiaansen et al., 2014), proteinuria (Goldwich et al., 2012), and lung inflammation (Chapman and Georas, 2013) as side effects of DT although molecular mechanisms underlying these phenotypes were unknown. These organ disorders and/or systemic disorders may affect HCs. DT ototoxicity was significant at P7 and P14 (Fig. 1 and 2), when the cochlea matures toward the onset of hearing by remodeling structures and changing gene expressions (Mikaelian and Ruben, 1965; Rubel and Fay, 2012; Walters and Zuo, 2013). DT could greatly affect HCs undergoing maturation in an indirect manner.

In conclusion, HCs are vulnerable cells that can be damaged by aging, environmental stress, infection, some ototoxic drugs, and also unknown factors (Furness, 2015). DT toxicity on HCs should be taken into consideration, and exploring the mechanisms is crucial for preventing HC loss. The existence of a critical period in DT toxicity may provide clues to address this issue. In addition, the present results demonstrate that phenotypes in otic or sound-associated behaviors should be interpreted with caution when researchers use the DT-DTR system in juvenile mice.

Acknowledgments

We are grateful to Mr. K. Itakura (Nagoya University Graduate School of Medicine) and Mr. H. Takase (Nagoya City University Graduate School of Medicine) for scanning electron microscopy, Mr. T. Yoshimoto for H&E staining, Ms. Y. Itai, and M. Okamoto for their technical assistance, and Ms. A. Asano for secretarial work. The scanning electron microscope was used in the Laboratory of Division for Medical Research Engineering, Nagoya University Graduate School of Medicine. This work was partly supported by KAKENHI (Grants-in-Aid for Scientific Research on Priority Areas “Brain Environment” 231111007 to H. Kiyama, “Grants-in-Aid for Young Scientist (B)” 25830050 and “Grant-in-Aid for Scientific Research (C)” 16K07055 to H. Konishi, and “Grants-in-Aid for Scientific Research on Innovative Areas” 16H01639 to N. O.) from the Ministry of Education, Culture, Sports, Science and Technology (MEXT) of Japan.

Author contributions

H. Konishi, N.O., T.N., S.U., K.Y., M.K and H. Kiyama designed the research. H. Konishi, N.O., A.M., Y.K., Y.A., M.K. performed the experiments. H. Konishi and H. Kiyama wrote the paper.

REFERENCES

Bonventre PF, Saelinger CB, Imhoff JG (1973) Studies on the effect of diphtheria toxin on protein synthesis in mice. J Med Microbiol 6:169-176.

Cha JH, Brooke JS, Eidels L (1998) Toxin binding site of the diphtheria toxin receptor: loss and gain of diphtheria toxin binding of monkey and mouse heparin-binding, epidermal growth factor-like growth factor precursors by reciprocal site-directed mutagenesis. Mol Microbiol 29:1275-1284.

Chapman TJ, Georas SN (2013) Adjuvant effect of diphtheria toxin after mucosal administration in both wild type and diphtheria toxin receptor engineered mouse strains. J Immunol Methods 400-401:122-126.

Christiaansen AF, Boggiatto PM, Varga SM (2014) Limitations of Foxp3(+) Treg depletion following viral infection in DEREG mice. J Immunol Methods 406:58-65.

Collier RJ, Kandel J (1971) Structure and activity of diphtheria toxin. I. Thiol-dependent dissociation of a fraction of toxin into enzymically active and inactive fragments. J Biol Chem 246:1496-1503.

Cox BC, Chai R, Lenoir A, Liu Z, Zhang L, Nguyen DH, Chalasani K, Steigelman KA, Fang J, Rubel EW, Cheng AG, Zuo J (2014) Spontaneous hair cell regeneration in the neonatal mouse cochlea in vivo. Development 141:816-829.

Dorland RB, Middlebrook JL, Leppla SH (1979) Receptor-mediated internalization and degradation of diphtheria toxin by monkey kidney cells. J Biol Chem 254:11337-11342.

Furness DN (2015) Molecular basis of hair cell loss. Cell Tissue Res 361:387-399.

Gill DM, Dinius LL (1971) Observations on the structure of diphtheria toxin. J Biol Chem 246:1485-1491.

Goldwich A, Steinkasserer A, Gessner A, Amann K (2012) Impairment of podocyte function by diphtheria toxin--a new reversible proteinuria model in mice. Lab Invest 92:1674-1685.

Han JH, Kushner SA, Yiu AP, Hsiang HL, Buch T, Waisman A, Bontempi B, Neve RL, Frankland PW, Josselyn SA (2009) Selective erasure of a fear memory. Science 323:1492-1496.

Honjo T, Nishizuka Y, Hayaishi O (1968) Diphtheria toxin-dependent adenosine diphosphate ribosylation of aminoacyl transferase II and inhibition of protein synthesis. J Biol Chem 243:3553-3555.

Hu L, Lu J, Chiang H, Wu H, Edge AS, Shi F (2016) Diphtheria Toxin-Induced Cell Death Triggers Wnt-Dependent Hair Cell Regeneration in Neonatal Mice. J Neurosci 36:9479-9489.

Hunter-Duvar IM (1978) A technique for preparation of cochlear specimens for assessment with the scanning electron microscope. Acta Otolaryngol Suppl 351:3-23.

Knowlton WM, Palkar R, Lippoldt EK, McCoy DD, Baluch F, Chen J, McKemy DD (2013) A sensory-labeled line for cold: TRPM8-expressing sensory neurons define the cellular basis for cold, cold pain, and cooling-mediated analgesia. J Neurosci 33:2837-2848.

Kurioka T, Lee MY, Heeringa AN, Beyer LA, Swiderski DL, Kanicki AC, Kabara LL, Dolan DF, Shore SE, Raphael Y (2016) Selective hair cell ablation and noise exposure lead to different patterns of changes in the cochlea and the cochlear nucleus. Neuroscience 332:242-257.

Kwon SJ, Lee GT, Lee JH, Iwakura Y, Kim WJ, Kim IY (2014) Mechanism of pro-tumorigenic effect of BMP-6: neovascularization involving tumor-associated macrophages and

IL-1a. Prostate 74:121-133.

Mahrt EJ, Perkel DJ, Tong L, Rubel EW, Portfors CV (2013) Engineered deafness reveals that mouse courtship vocalizations do not require auditory experience. J Neurosci 33:5573-5583.

Meyer Zu Horste G, Zozulya AL, El-Haddad H, Lehmann HC, Hartung HP, Wiendl H, Kieseier BC (2010) Active immunization induces toxicity of diphtheria toxin in diphtheria resistant mice--implications for neuroinflammatory models. J Immunol Methods 354:80-84.

Mikaelian D, Ruben RJ (1965) Development of hearing in the normal Cba-J mouse: correlation of physiological observations with behavioral responses and with cochlear anatomy. Acta oto-laryngologica 59:451-461.

Mitamura T, Higashiyama S, Taniguchi N, Klagsbrun M, Mekada E (1995) Diphtheria toxin binds to the epidermal growth factor (EGF)-like domain of human heparin-binding EGF-like growth factor/diphtheria toxin receptor and inhibits specifically its mitogenic activity. J Biol Chem 270:1015-1019.

Naglich JG, Metherall JE, Russell DW, Eidels L (1992) Expression cloning of a diphtheria toxin receptor: identity with a heparin-binding EGF-like growth factor precursor. Cell 69:1051-1061.

Nakashima T, Pyykko I, Arroll MA, Casselbrant ML, Foster CA, Manzoor NF, Megerian CA, Naganawa S, Young YH (2016) Meniere's disease. Nat Rev Dis Primers 2:16028.

Noben-Trauth K, Zheng QY, Johnson KR (2003) Association of cadherin 23 with polygenic inheritance and genetic modification of sensorineural hearing loss. Nat Genet 35:21-23.

Ohgami N, Ida-Eto M, Shimotake T, Sakashita N, Sone M, Nakashima T, Tabuchi K, Hoshino

T, Shimada A, Tsuzuki T, Yamamoto M, Sobue G, Jijiwa M, Asai N, Hara A, Takahashi M, Kato M (2010) c-Ret-mediated hearing loss in mice with Hirschsprung disease. Proc Natl Acad Sci U S A 107:13051-13056.

Ohlemiller KK, Dahl AR, Gagnon PM (2010) Divergent aging characteristics in CBA/J and CBA/CaJ mouse cochleae. J Assoc Res Otolaryngol 11:605-623.

Pappenheimer AM, Jr., Harper AA, Moynihan M, Brockes JP (1982) Diphtheria toxin and related proteins: effect of route of injection on toxicity and the determination of cytotoxicity for various cultured cells. J Infect Dis 145:94-102.

Parker M, Brugeaud A, Edge AS (2010) Primary culture and plasmid electroporation of the murine organ of Corti. J Vis Exp.

Parkhurst CN, Yang G, Ninan I, Savas JN, Yates JR, 3rd, Lafaille JJ, Hempstead BL, Littman DR, Gan WB (2013) Microglia promote learning-dependent synapse formation through brain-derived neurotrophic factor. Cell 155:1596-1609.

Patuzzi R (2011) Ion flow in stria vascularis and the production and regulation of cochlear endolymph and the endolymphatic potential. Hear Res 277:4-19.

Pedersen J, Ugleholdt RK, Jorgensen SM, Windelov JA, Grunddal KV, Schwartz TW, Fuchtbauer EM, Poulsen SS, Holst PJ, Holst JJ (2013) Glucose metabolism is altered after loss of L cells and alpha-cells but not influenced by loss of K cells. Am J Physiol Endocrinol Metab 304:E60-73.

Robinson EA, Henriksen O, Maxwell ES (1974) Elongation factor 2. Amino acid sequence at the site of adenosine diphosphate ribosylation. J Biol Chem 249:5088-5093.

Rubel EW, Fritzsch B (2002) Auditory system development: primary auditory neurons and their targets. Annu Rev Neurosci 25:51-101.

Rubel EW, Fay RR (2012) Development of the auditory system: Springer Science & Business Media.

Saito M, Iwawaki T, Taya C, Yonekawa H, Noda M, Inui Y, Mekada E, Kimata Y, Tsuru A, Kohno K (2001) Diphtheria toxin receptor-mediated conditional and targeted cell ablation in transgenic mice. Nat Biotechnol 19:746-750.

Schecterson LC, Bothwell M (1994) Neurotrophin and neurotrophin receptor mRNA expression in developing inner ear. Hear Res 73:92-100.

Song Y, Xia A, Lee HY, Wang R, Ricci AJ, Oghalai JS (2015) Activity-dependent regulation of prestin expression in mouse outer hair cells. J Neurophysiol 113:3531-3542.

Tong L, Strong MK, Kaur T, Juiz JM, Oesterle EC, Hume C, Warchol ME, Palmiter RD, Rubel EW (2015) Selective deletion of cochlear hair cells causes rapid age-dependent changes in spiral ganglion and cochlear nucleus neurons. J Neurosci 35:7878-7891.

Walters BJ, Zuo J (2013) Postnatal development, maturation and aging in the mouse cochlea and their effects on hair cell regeneration. Hear Res 297:68-83.

Wang H, Melton DW, Porter L, Sarwar ZU, McManus LM, Shireman PK (2014) Altered macrophage phenotype transition impairs skeletal muscle regeneration. Am J Pathol 184:1167-1184.

Wang J, Tymczyszyn N, Yu Z, Yin S, Bance M, Robertson GS (2011) Overexpression of X-linked inhibitor of apoptosis protein protects against noise-induced hearing loss in mice. Gene Ther 18:560-568.

Willott JF (1986) Effects of aging, hearing loss, and anatomical location on thresholds of inferior colliculus neurons in C57BL/6 and CBA mice. J Neurophysiol 56:391-408.

Xu M, Kobets A, Du JC, Lennington J, Li L, Banasr M, Duman RS, Vaccarino FM, DiLeone

RJ, Pittenger C (2015) Targeted ablation of cholinergic interneurons in the dorsolateral striatum produces behavioral manifestations of Tourette syndrome. Proc Natl Acad Sci U S A 112:893-898.

Zhang F, Dai M, Neng L, Zhang JH, Zhi Z, Fridberger A, Shi X (2013) Perivascular macrophage-like melanocyte responsiveness to acoustic trauma--a salient feature of strial barrier associated hearing loss. Faseb J 27:3730-3740.

Zhang J, Chen S, Hou Z, Cai J, Dong M, Shi X (2015) Lipopolysaccharide-induced middle ear inflammation disrupts the cochlear intra-strial fluid-blood barrier through down-regulation of tight junction proteins. PLoS One 10:e0122572.

Zhang W, Dai M, Fridberger A, Hassan A, Degagne J, Neng L, Zhang F, He W, Ren T, Trune D, Auer M, Shi X (2012) Perivascular-resident macrophage-like melanocytes in the inner ear are essential for the integrity of the intrastrial fluid-blood barrier. Proc Natl Acad Sci U S A 109:10388-10393.

FIGURE LEGENDS

Fig. 1. Permanent hearing loss in C57BL/6 mice administrated with DT at P7.

(A) Representative ABR waveforms at 0, 20, 40, 60, and 80 db SPL of 12 kHz sound in P21. No waveform was observed under 60 dB SPL in DT-administrated mice. **(B)** ABR threshold of 4, 12, 20, and 32 kHz sounds at P21 (PBS: n = 4; DT: n = 5). #: number of scale-out animals. *P < 0.05, **P < 0.001; two-tailed unpaired Student's *t*-test. **(C)** ABR threshold of 4, 12, 20, and 32 kHz sounds at 8W (PBS: n = 4; DT: n = 5). The same animals used in **B** were allowed to mature to 8W and analyzed. #: number of scale-out animals. *P < 0.05, **P < 0.001; two-tailed unpaired Student's *t*-test.

Fig. 2. Juvenile C57BL/6 mice are vulnerable to DT.

ABR threshold of 4, 12, 20, and 32 kHz sounds at 14 or 15 days after PBS and DT administration. **(A)** Administration at P14 and analysis at P28 (PBS: n = 5; DT: n = 5). #: number of scale-out animals. *P < 0.05, **P < 0.001; two-tailed unpaired Student's *t*-test. **(B)** Administration at P28 and analysis at P43 (PBS: n = 5; DT: n = 5). No significance was observed at all frequencies. **(C)** Administration at 8W and analysis at 10W (14 days later) (PBS: n = 5; DT: n = 5). No significance was observed at all frequencies.

Fig. 3. Degeneration of SGNs and HCs after DT administration at P7 in C57BL/6 mice.

(A) Sections of the cochlear middle turn with H&E staining at P21 and 8W. Insets show higher magnifications of the organ of Corti. An arrow and an arrowhead indicate IHC and OHC, respectively. Scale bar = 100 µm and 30 µm (insets). **(B)** Density of SGNs in the apical, middle and basal turn at P21 and 8W (n = 3). Values show mean ± S.E.M. *P < 0.05, **P < 0.005;

two-tailed unpaired Student's *t*-test. **(C)** Whole-mount TNBT staining of HCs in the apical, middle and basal turn at P21. Scale bar = 50 μm **(D)** Number of IHCs and OHCs in apical, middle, and basal turn of cochlea at P21 (n = 5). Values show mean ± S.E.M. $^*P < 0.05$, $^{**}P < 0.001$; two-tailed unpaired Student's *t*-test. **(E)** IHC and OHC degeneration in the middle turn determined by SEM. Arrows show degenerated HCs. Scale bar = 10 μm.

Fig. 4. Time-course of HC degeneration in the middle turn of C57BL/6 mice.

Mice administered with PBS **(A–C, G–I and M–O)** and DT **(D–F, J–L and P–R)** at P7 were analyzed by SEM at P8 **(A–F)**, P10 **(G–L)** and P14 **(M–R)**. Areas indicated by red squares were shown as higher magnification images. Higher magnification of IHCs: **B**, **E**, **H**, **K**, **N** and **Q**. Higher magnification of OHCs: **C**, **F**, **I**, **L**, **O** and **R**. Arrows show degenerated HCs. An arrowhead in **J** (shown in **L** as a high magnification image) shows a putative degenerating cell. Scale bar = 10 μm **(A, D, G, J, M and P)** and 2 μm **(B, C, E, F, H, I, K, L, N, O, Q and R)**.

Fig. 5. DT ototoxicity in juvenile CBA/J mice.

CBA/J mice administered PBS and DT at P7 were analyzed at P21. **(A)** ABR threshold of 4, 12, 20, and 32 kHz sounds (PBS: n = 4; DT: n = 5). Note that there were no scale-out animals in contrast to Fig. 1. $^*P < 0.05$, $^{**}P < 0.001$; two-tailed unpaired Student's *t*-test. **(B)** IHC and OHC degeneration in the middle turn as determined by SEM. Arrows show degenerated HCs. Scale bar = 10 μm.

Figure 1
Click here to download high resolution image

Figure 1. Konishi et al.

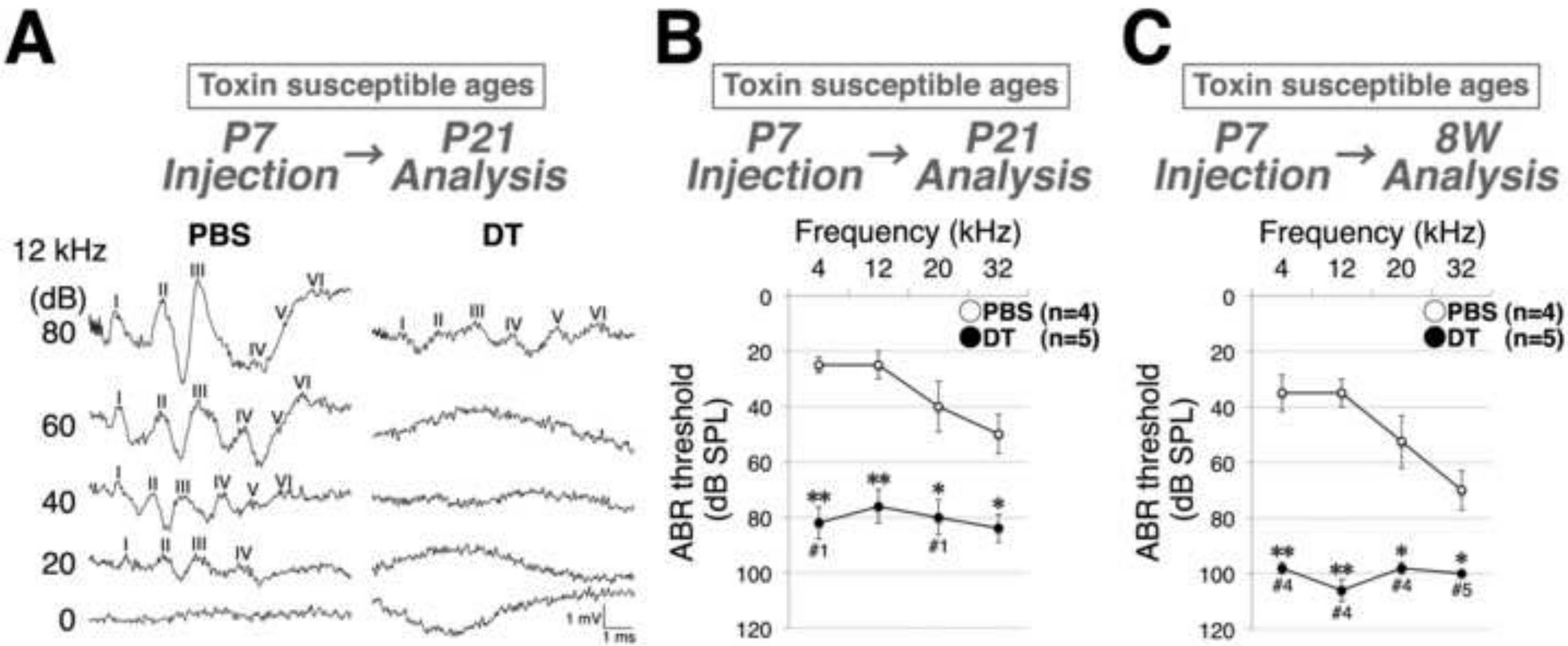

Figure 2
Click here to download high resolution image

Figure 2. Konishi et al.

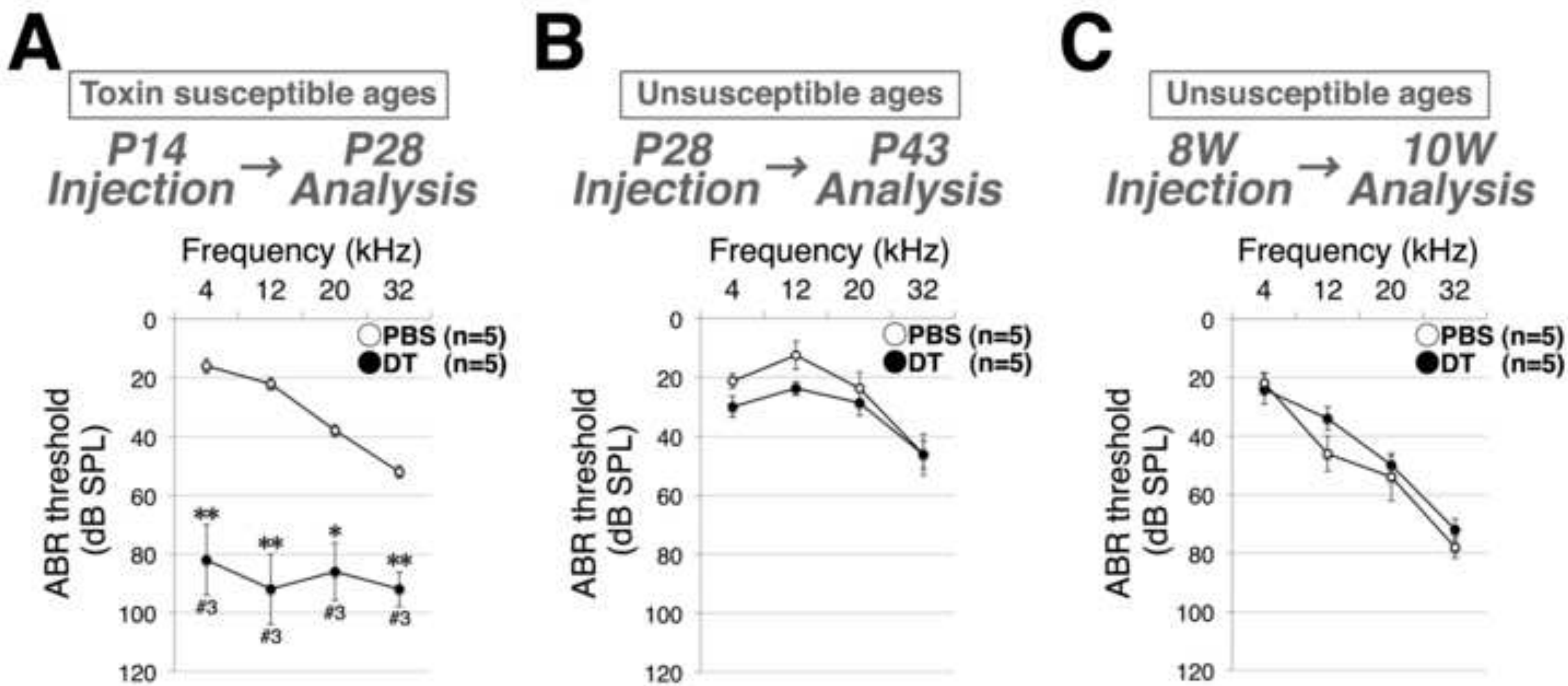

Figure 3
Click here to download high resolution image

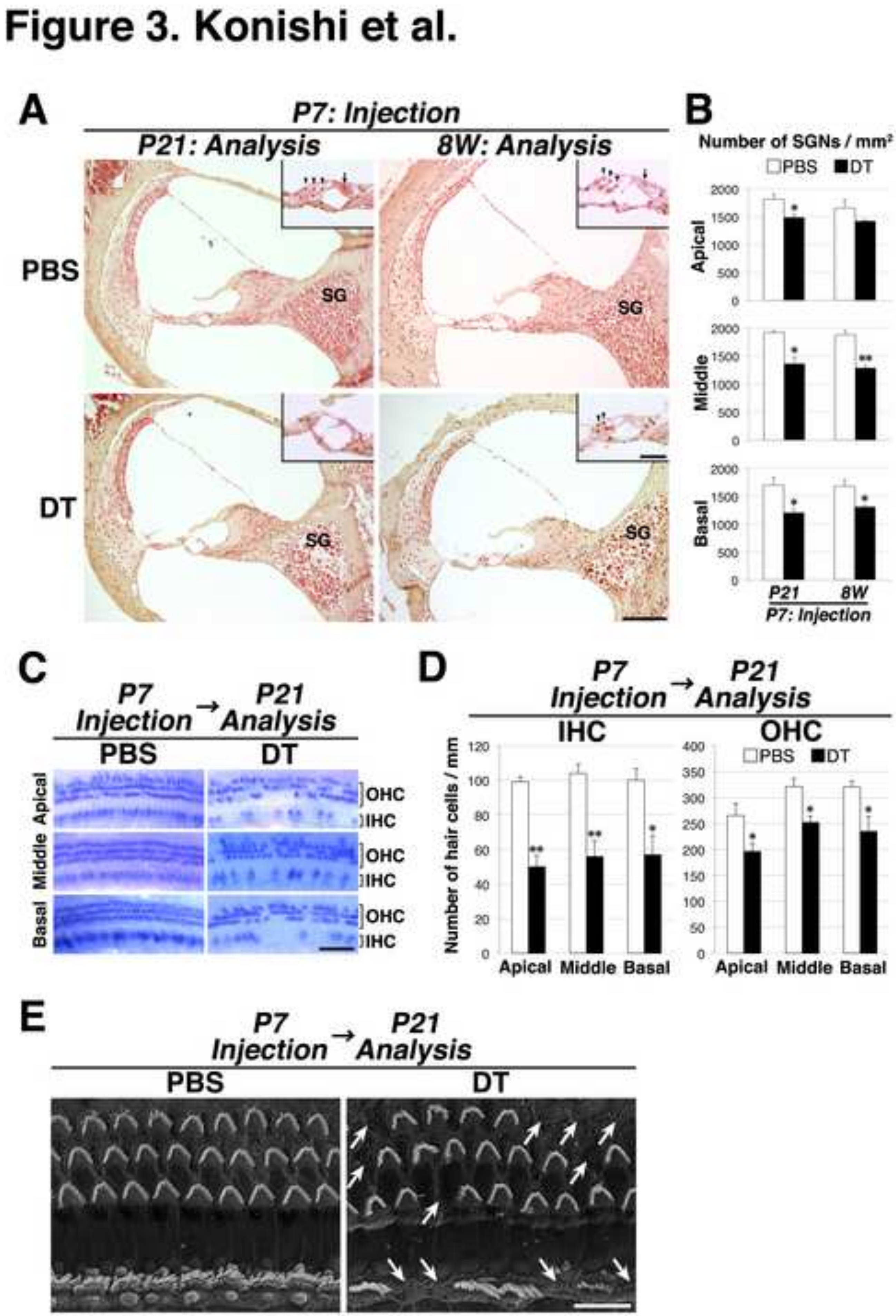

Figure 4
Click here to download high resolution image

Figure 4. Konishi et al.

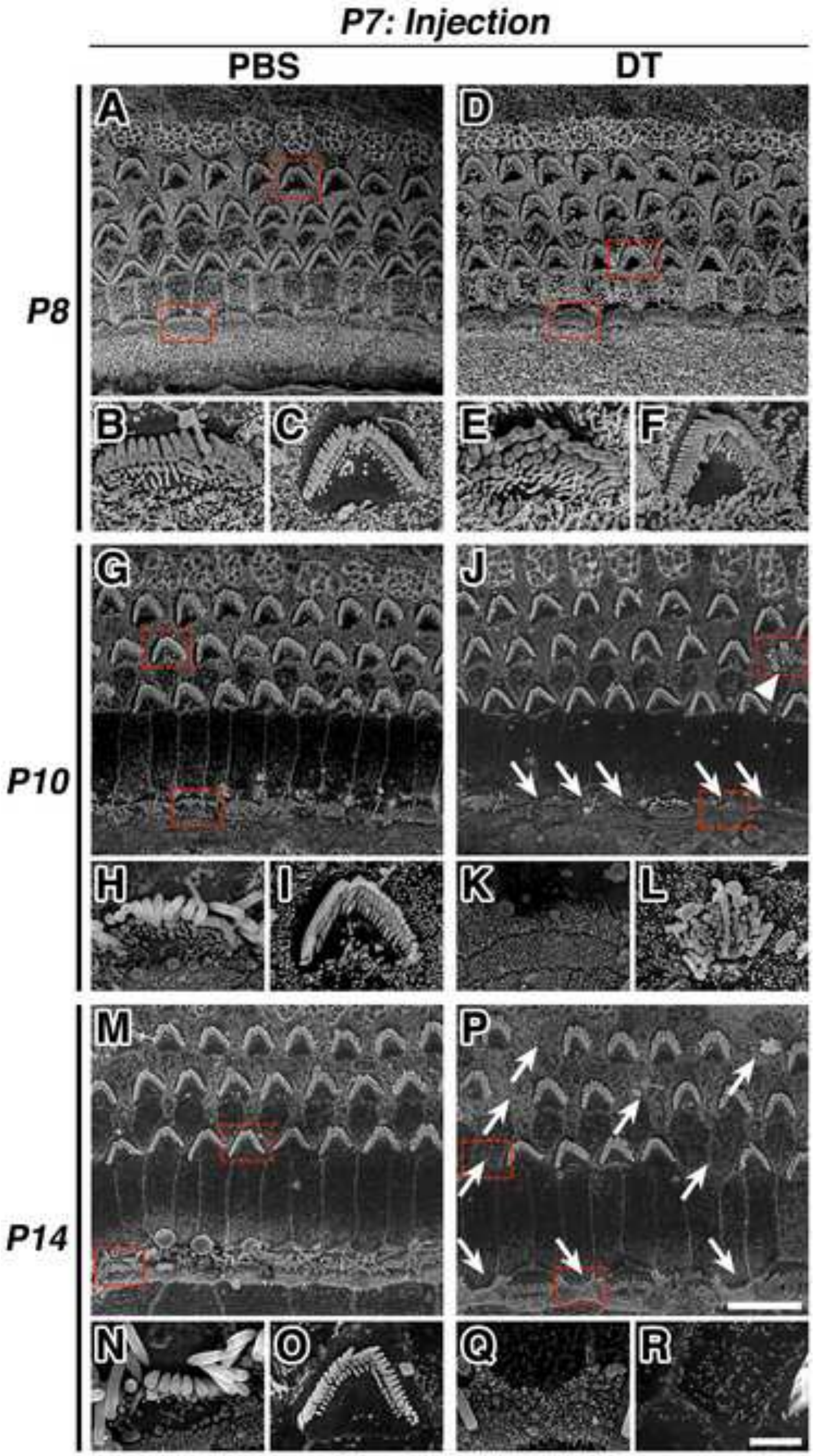

Figure 5
Click here to download high resolution image

Figure 5. Konishi et al.